Clinical and Experimental Medicine (2024) 24:243
https://doi.org/10.1007/s10238-024-01510-0

RESEARCH

SASS6 promotes tumor proliferation and is associated with TP53 and immune infiltration in lung adenocarcinoma

Zihao Li[1] · Lingyun He[1] · Jiayi Li[2] · Jing Qian[3] · Zuotao Wu[3] · Yongjie Zhu[3] · Ting Zhuo[4] · Jusen Nong[5] · Honghua Liang[1] · Hua Zheng[1] · Weijia Huang[1] · Julu Huang[6] · Jianbin Cao[1]

Received: 15 June 2024 / Accepted: 16 October 2024 / Published online: 24 October 2024

Abstract

The most common type of non-small cell lung cancer is lung adenocarcinoma (LUAD), which is characterized by high morbidity and poor survival. Up-regulation of SASS6 expression can lead to the progression of various malignant tumors. However, there are no relevant studies on the role of SASS6 in LUAD. SASS6 was highly expressed in most tumors, reflecting a good diagnostic value, and its overexpression in LUAD indicated discouraging overall prognosis. Functional enrichment analysis suggested that SASS6 was associated with cell cycle in LUAD. In addition, patients with high SASS6 expression had worse immune infiltration, but higher TMB and immune checkpoint, and higher sensitivity to multiple targeted drugs such as osimertinib. Cell experiments confirmed that knockdown of SASS6 could inhibit the viability of tumor cells.SASS6 has important value in the diagnosis of cancer. In particular, SASS6 is a crucial factor in the progression of LUAD, and has important clinical value, especially in the diagnosis, prognosis and treatment

Keywords Cell cycle · Immune infiltration · Lung adenocarcinoma · Prognosis · SASS6

Introduction

Worldwide, NSCLC is a major challenge to human health and a serious threat to life, while LUAD accounts for about 80% of lung cancers [1, 2]. The five-year survival rate of patients with NSCLC is closely related to the pathological stage of the tumor, and the five-year survival rate of patients with early stage is about 80%, while advanced cases with metastasis is even less than 10% [3]. LUAD has the important characteristics of high incidence and low survival rate. Radical resection is an effective treatment for early NSCLC, but the rapid development of targeted therapy and immunotherapy in recent years has brought tremendous changes and effects on the treatment of advanced cases [4, 5]. TP53, EGFR, and KRAS are the most frequently mutated genes in LUAD, and the treatment mode developed based on these mutated genes is targeted therapy, among which EGFR-TKI is the most familiar,

Zihao Li, Lingyun He and Jiayi Li have contributed equally to this work.

✉ Julu Huang
huangjulu@stu.gxmu.edu.cn

✉ Jianbin Cao
18907722555@163.com

[1] Department of Thoracic Surgery, Liuzhou People's Hospital affiliated to Guangxi Medical University, Liuzhou, Guangxi, China

[2] Department of Nephrology, Liuzhou People's Hospital affiliated to Guangxi Medical University, Liuzhou, Guangxi, China

[3] Department of Cardio-Thoracic Surgery, The First Affiliated Hospital of Guangxi Medical University, Nanning, Guangxi, China

[4] Department of Respiratory Medicine, The First Affiliated Hospital of Guangxi Medical University, Nanning, Guangxi, China

[5] Department of Pediatric Surgery, The First Affiliated Hospital of Guangxi Medical University, Nanning, Guangxi, China

[6] Department of Medical Oncology, Liuzhou People's Hospital affiliated to Guangxi Medical University, Liuzhou, Guangxi, China

and these drugs include afatinib, erlotinib, gefitinib, and osimertinib [6, 7]. Immune checkpoint genes is closely related to the homeostasis of the tumor immune microenvironment, and immune checkpoint inhibitors have been widely used as a means of immunotherapy [8]. Acquired drug resistance is the main challenge that restricts the long-term effect of these two therapeutic approaches [9]. The exploration of molecular biomarkers is one of the effective ways to improve the early diagnosis and accurate treatment of lung adenocarcinoma.

Spindle assembly abnormal protein 6 homolog (SASS6) plays a part in the regulation of the number of centrosomes in human cells and is a crucial protein required for centrosome replication [10]. The centrosome regulates the progression of human cell mitosis, and the abnormality of centrosome can cause the disorder of cell cycle and chromosome instability, which is closely related to the occurrence and progression of tumor [11–13]. Previous studies have confirmed that SASS6 is overexpressed in breast cancer, and knocking down SASS6 inhibits the growth of tumor cells [14]. SASS6 expression is upregulated in esophageal squamous cell carcinoma, and studies have shown that the promotion of esophageal cancer proliferation is achieved by inhibiting the p53 signaling pathway [15]. However, there are no relevant studies on the role of SASS6 in LUAD. Therefore, the relationship between the expression of SASS6 and LUAD was investigated in this study.

Materials and methods

Data acquisition

The cancer genome atlas (TCGA) datasets were downloaded from UCSC Xena (xenabrowser.net), including pan-cancer dataset, prognostic data and gene expression profiles of LUAD patients. GSE27262, GSE30219, GSE43458, and GSE198291 were obtained from gene expression omnibus (GEO) (https://www.ncbi.nlm.nih.gov/geo/). Data had been converted by log2(x + 1). Through the use of Genomic Data Commons (https://portal.gdc.cancer.gov/) from the TCGA obtained simple nucleotide variation data.

Comparison of SASS6 expression at RNA and protein levels

We used Student's t-test to analyze and compare SASS6 expression differences between a variety of human cancer tumor samples and adjacent non-tumor samples, especially in LUAD. At the protein expression level, validation of the difference in SASS6 expression was performed using UALCAN (https://ualcan.path.uab.edu/) and Human Protein Atlas (HPA) database (http://www.proteinatlas.org/).

Analysis of SASS6 expression at the level of single cell sequencing

The quality control procedure of GSE198291 was performed with R package Seurat. Reduction of dimensionality and clustering were implemented through uniform manifold approximation and projection (UMAP). The cells were annotated according to marker genes using CellMarker database.

Analysis of diagnostic efficiency

SASS6 expression was extracted to distinguish tumors from normal samples, and the receiver operator characteristic (ROC) curve was established using R package ROCR.

Survival and prognosis analysis

Kaplan–Meier (KM) method was applied to draw survival curve. The above procedure was implemented by loading the R package survival and survminer. Cross-validation of the survival analysis was performed by using GEPIA database (http://gepia.cancer-pku.cn/). The cut-off value for grouping using SASS6 expression levels was 50% ((high and low SASS6 groups).

Differential expression genes (DEGs)

LUAD cases were divided into two groups (high and low SASS6 groups), and they were analyzed by R package limma to obtain DEGs associated with SASS6. Set the threshold for filtering DEGs to the absolute value of log2foldchange ≥ 1.0.

Functional enrichment analysis

To investigate the potential functional mechanisms of SASS6 in LUAD, we implemented gene ontology (GO), Kyoto encyclopedia of genes and genomes (KEGG), and gene set enrichment analysis (GSEA) on DEGs by R package clusterProfiler.

Analysis of immune cell infiltration

TIMER (https://cistrome.shinyapps.io/timer/) was applied to analyze the relationship between immune cells and genes [16]. The influence of SASS6 copy number variation on the immune infiltration was investigated by using TIMER database. R package GSVA was applied to quantify the expression levels of immune cells in tumor cases, and immune cell

expression was compared between two groups with different SASS6 expression (ssGSEA). R package estimate was loaded to assess the microenvironment composition of each tumor case, and stromal scores, immune scores, ESTIMATE scores, and tumor purity were inferred for all tumor cases, and these results were subsequently analyzed and compared (ESTIMATE).

Association of SASS6 with gene mutation and immune checkpoint expression

Tumor cases were divided into two groups, and R package maftools was loaded to map the waterfall plots of gene mutations in the two groups respectively. Finally, TMB and immune checkpoint gene between the two groups were compared, respectively.

Drug sensitivity

We applied R packet oncoPredict to predict the sensitivity of each tumor sample to a number of drugs. The drug sensitivity between the two groups (high and low SASS6 groups) was compared.

Construction of ceRNA network of SASS6

The ENCORI database (https://rnasysu.com/encori/index.php) was applied to predict relevant miRNAs and lncRNAs, and the correlation analysis was further verified. According to the ceRNA theory, predicted miRNAs inversely correlated with SASS6 (Spearman coefficient $r < -0.3$, $p < 0.05$) were considered miRNAs targeted SASS6, and predicted lncRNAs inversely correlated with miRNA (Spearman coefficient $r < -0.3$, $p < 0.05$) were considered lncRNAs targeted miRNA. Core miRNA and core lncRNA meet the conditions that their expression differ between tumor and normal cases and affect the prognosis of tumor cases.

Acquisition of LUAD specimens from humans

The paraffin-embedded specimens of 4 patients with LUAD, including cancer and adjacent tissues, were acquired from the First Affiliated Hospital of Guangxi Medical University.

Immunohistochemistry

The tissue specimens were formaldehyde-fixed and paraffin-embedded followed by cutting into sections. Following the instructions of a commonly used two-step, immunohistochemical staining was performed on each tissue. The tissue sections were incubated with the anti SASS6 (1:200) overnight at 4 °C. They were then incubated for 30 min with the enhanced enzyme labeled goat anti mouse/rabbit IgG polymer. Finally, the tissue sections were stained using a DAB chromogenic kit (ZLI-9018, ZSGB-Bio, China) and counterstained with hematoxylin.

Cell lysate preparation

For cytoplasmic protein extraction, RIPA Lysis buffer containing 1% PMSF (both from Beyotime) was used to lyse the cells. The protein concentration was determined before adding buffer and boiling for 10 min prior to storage at − 80 °C.

Western blot

For electrophoresis on an SDS-PAGE gel with an 8% concentration per lane, we loaded samples containing approximately 25 µg protein onto it before transferring them onto a PVDF membrane from Sigma Aldrich in the USA. Incubation overnight at a temperature of 4 °C was done after applying primary antibodies. The primary antibodies used included E-Cadherin (#20,874-1-AP; Proteintech), N-Cadherin (#22,018-1-AP; Proteintech), Vimentin (#abs171412; absin), Pan-Cytokeratin (#BH0149; Bioss), and SASS6 (#21,377-1-A; Proteintech). β-Actin (#81,115-1-RR; Proteintech) was used for normalization.

Cell proliferation

Cell proliferation assays were conducted using the Cell counting kit-8 (CCK-8; Beyotime) and BeyoClickTM EdU-555 Cell Proliferation Detection Kit (EdU; Beyotime). After 24 h of transfection, the cells were treated with EdU solution and observed under a fluorescence microscope (EVOS M7000, Thermo Fisher Scientific, USA) for imaging purposes. Additionally, CCK-8 solution was introduced at 24, 48, 72 h followed by measuring the absorbance at a wavelength of 450 nm.

Wound healing assay

The six-well plate was used for cell inoculation, and once the cell density reached approximately 80–90%, a sterile needle 10 µL was employed to create a vertical wound. Microscopic imaging of the same region was conducted twice, at both 0 h and 24 h respectively, using a Nikon Japan microscope.

Transwell assay

Migration and invasion assays were implemented using transwell chambers (LABSELECT, China) with 8 µm pore size. Cells harvested 24 h after transfection were resuspended and added to the upper chamber at a volume of 250µL, 700µL

of medium containing 10% FBS in the lower chamber, and placed in the incubator for 36 h.

Statistical analysis

Statistics were performed by R, version 4.2.3. The differential expression between the two groups was analyzed by t-test. The log-rank test was used for KM survival analysis. The correlation analysis employed Spearman's correlation to evaluate. The threshold of significant difference was set as $p<0.05$ (ns, $p>0.05$; *, $p<0.05$; **, $p<0.01$; ***, $p<0.001$).

Results

Differential expression of SASS6 between tumor and normal cases

Pan-cancer analysis demonstrated that SASS6 was overexpressed in tumor samples compared to adjacent tissues in multiple types of cancer in the TCGA database (Fig. 1A). The area under the ROC curve of bladder cancer (BLCA), cervical cancer (CESC), cholangiocarcinoma (CHOL), colon adenocarcinoma (COAD), esophageal cancer (ESCA), glioblastoma (GBM), head and neck squamous cancer (HNSC), liver hepatocellular carcinoma (LIHC), lung squamous cell carcinoma (LUSC), stomach adenocarcinoma (STAD), and uterine corpus endometrial carcinoma (UCEC) were all greater than 0.8, indicating that SASS6 had good diagnostic efficacy for pan-cancer (Fig. 1B–L).

Differential analysis of SASS6 expression in LUAD

Analysis of the TCGA and GEO validation datasets demonstrated that, compared with normal lung tissue, the expression of SASS6 at the RNA expression level was up-regulated in LUAD (Fig. 2A–C). Analysis results from the UALCAN and HPA databases revealed that SASS6 was overexpressed in LUAD at the protein expression level (Fig. 2D–F). SASS6 expression tended to be higher in groups with a high clinical T stage in LUAD (Fig. 2G). SASS6 expression was upregulated in patients with an advanced pathological stage (Fig. 2H).

Comparison of SASS6 expression in multiple cell clusters

The heat map listed the top 10 marker genes for all cell clusters (Fig. 3A). The types of cell clusters were annotated separately according to the marker genes of each cell cluster, which included ciliated cell, megakaryocyte, idiopathic pulmonary fibrosis (IPF) cell, T cell, cancer stem cell, epithelial cell, type II pneumocyte, secretory cell, and mesenchymal stromal cell (MSC) (Fig. 3B). Comparison of SASS6 expression in these cell clusters revealed that SASS6 was mainly expressed in cancer stem cells and mesenchymal stromal cells (Fig. 3C).

Diagnostic value and survival analysis of SASS6 in LUAD

The expression of SASS6 was extracted to distinguish LUAD from normal samples, and ROC curves were constructed to evaluate the efficiency of discrimination. The area under ROC curves from TCGA, GSE27262 and GSE43458 were 0.8968, 0.7856 and 0.7413, respectively (Fig. 4A–C). The above results confirmed the excellent diagnostic value of SASS6 in LUAD. Survival analyses from the TCGA, GSE30219 dataset, and GEPIA database demonstrated a worse prognosis for LUAD patients with high SASS6 expression (Fig. 4D–F).

Identification of DEGs related to SASS6 and functional enrichment analysis based on DEGs

Through the analysis of tumor cases with different SASS6 expression, the obtained DEGs included 804 up-regulated DEGs and 469 down-regulated DEGs (Fig. 5A). GO analysis showed that the biological processes were all related to the cell cycle, including "nuclear division", "chromosome segregation", and "nuclear chromosome segregation" (Fig. 5B). KEGG analysis enriched DEGs in multiple items, of which the most significant were "Neuroactive ligand – receptor interaction", "Cell cycle", "Oocyte meiosis", "Salivary secretion", "Nicotine addiction" (Fig. 5C). GSEA analysis enriched DEGs in these items, which were "GO_CARBOHYDRATE_BINDING", "GO_CELL_CYCLE", "GO_CELL_SURFACE", "GO_DIGESTION", "GO_DNA_BINDING_TRANSCRIPTION_FACTOR_ACTIVITY", "GO_IMMUNE_EFFECTOR_PROCESS", "GO_POSITIVE_REGULATION_OF_IMMUNE_RESPONSE", "GO_REGULATION_OF_IMMUNE_RESPONSE", "GO_REGULATION_OF_IMMUNE_SYSTEM_PROCESS", and "GO_VACUOLE" (Fig. 5D).

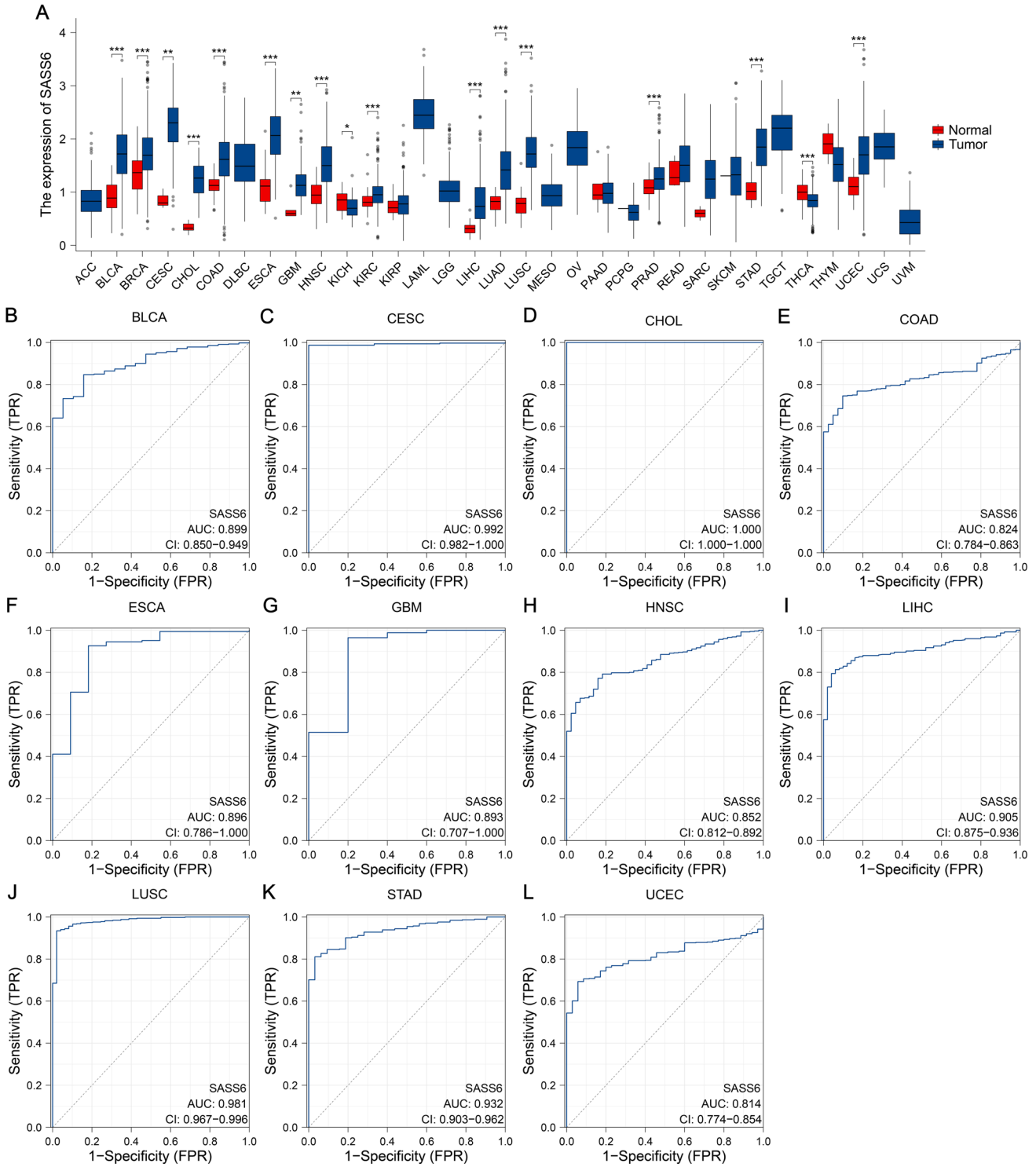

Fig. 1 Differential expression and diagnostic value of SASS6 in pan-cancer. **A** Analysis of SASS6 expression in pan-cancer from the TCGA dataset. **B–L** Diagnostic ROC curves constructed in relation to SASS6 expression in BLCA, CESC, CHOL, COAD, ESCA, GBM, HNSC, LIHC, LUSC, STAD, and UCEC

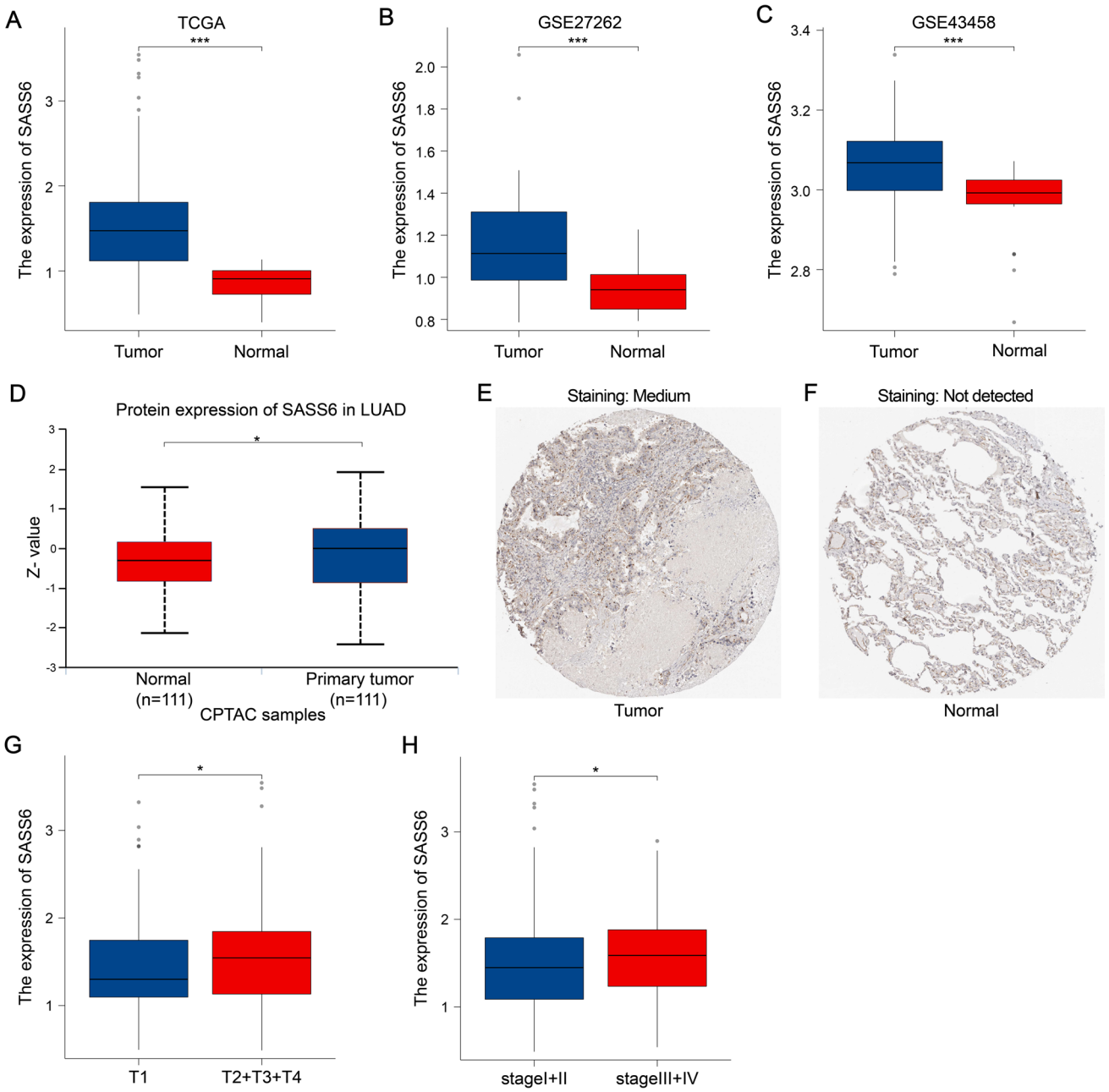

Fig. 2 **A–C** Comparison of SASS6 expression differences in TCGA, GSE27262, and GSE43458 datasets. **D** Comparison of protein levels of SASS6 from the UALCAN database. **E–F** Immunohistochemical staining of SASS6 in LUAD and lung tissue from the HPA database. **G** Comparison of SASS6 expression in LUAD between the different T stages. **H** Comparison of SASS6 expression in LUAD between the different pathological stages

Analysis of immune cell infiltration in tumor cases with different SASS6 expression

Samples with increased or decreased arm-level of SASS6 in LUAD showed decreased infiltration of a variety of immune cells, including B cell, CD8+ T cell, CD4+ T cell, Macrophage, neutrophil (Fig. 6A). Samples with high SASS6 expression had 16 subtypes of immune cells that were low expressed (Activated B cell, Activated dendritic cell, CD56dim natural killer cell, Central memory CD4 T cell, Eosinophil, Immature B cell, Macrophage, Mast cell, MDSC, Monocyte, Natural killer cell, Neutrophil, Plasmacytoid dendritic cell, T follicular helper cell, Type 1 T helper cell, and Type 17 T helper cell) and 4 subtypes of immune cells that were high expressed (Fig. 6B). In addition, the samples with high SASS6 expression had

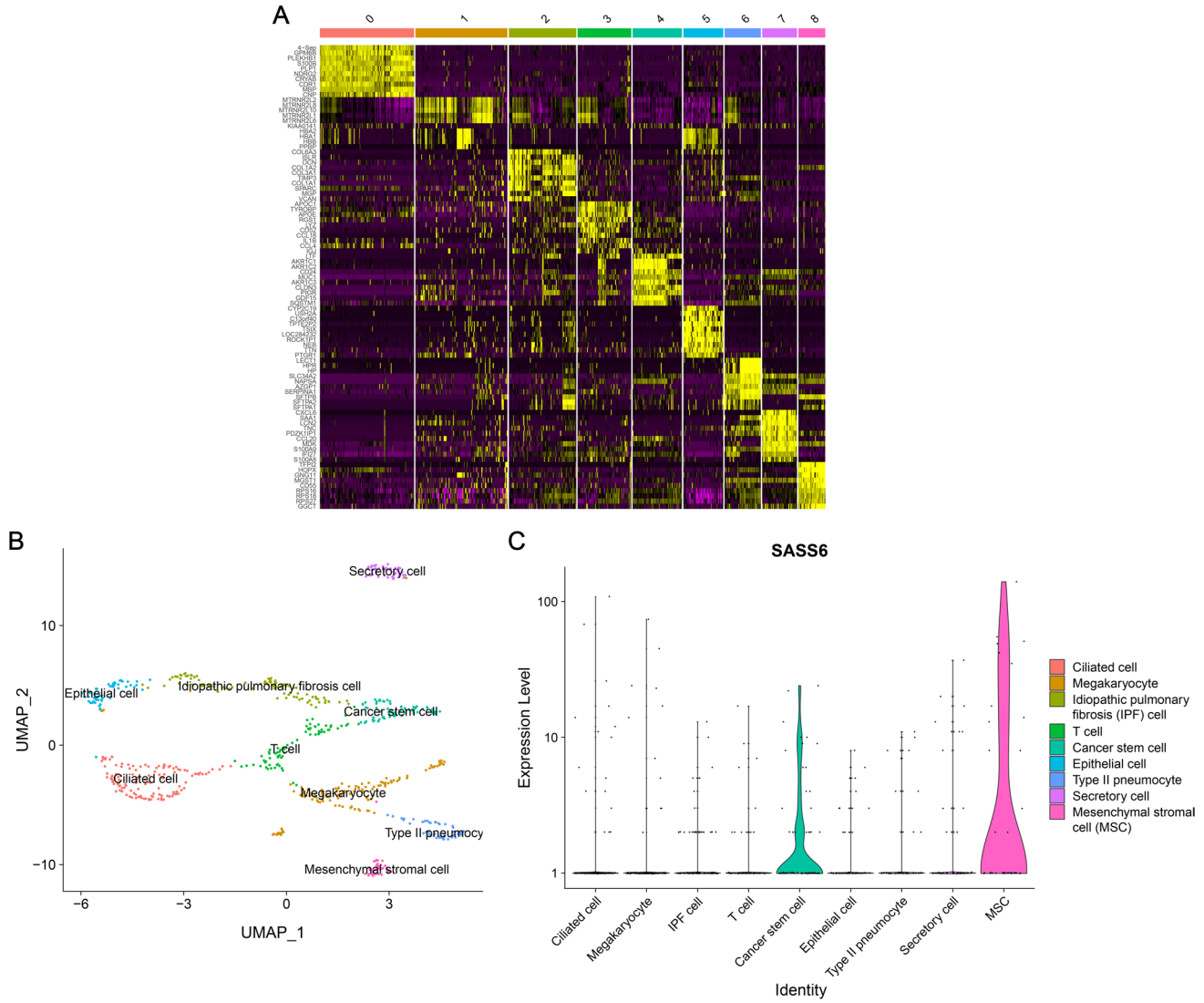

Fig. 3 Annotation of cell types and analysis of SASS6 expression. **A** Heat map of expression of marker genes in multiple cell clusters from LUAD tissue. **B** UMAP map of dimensionality reduction and cell clustering. **C** Comparison of SASS6 expression in multiple cell clusters

lower ESTIMATE, Immune, and Stromal scores but higher tumor purity (Fig. 6C).

Differences in TMB and immune checkpoint expression between the two groups

Immune checkpoint and TMB had an impact on immunotherapy in tumor patients, and then we analyzed the relationship between SASS6 and them to explore the role of SASS6 in immunotherapy. As shown in the two waterfall maps of gene mutations from the two groups with different SASS6 expression, there were more TP53 mutation cases in high SASS6 expression group, and more than 70% of patients in the high SASS6 expression group had TP53 mutations, while TP53 mutations in low SASS6 expression group was only 25% (Fig. 7A, B). The expression of PDCD1, CD274, PDCD1LG2, LAG3 and the value of TMB were all higher in the samples with high SASS6 expression (Fig. 7C, D).

Analysis of the relationship between SASS6 and drug sensitivity

There was lower half-maximal inhibitory concentration (IC50) of afatinib, crizotinib, erlotinib, gefitinib, osimertinib, savolitinib, cisplatin, cyclophosphamide, docetaxel, paclitaxel, vincristine, and vinorelbine in the high SASS6 expression group, suggesting that LUAD patients with high SASS6 expression may be more sensitive to the drugs mentioned above (Fig. 8A–L).

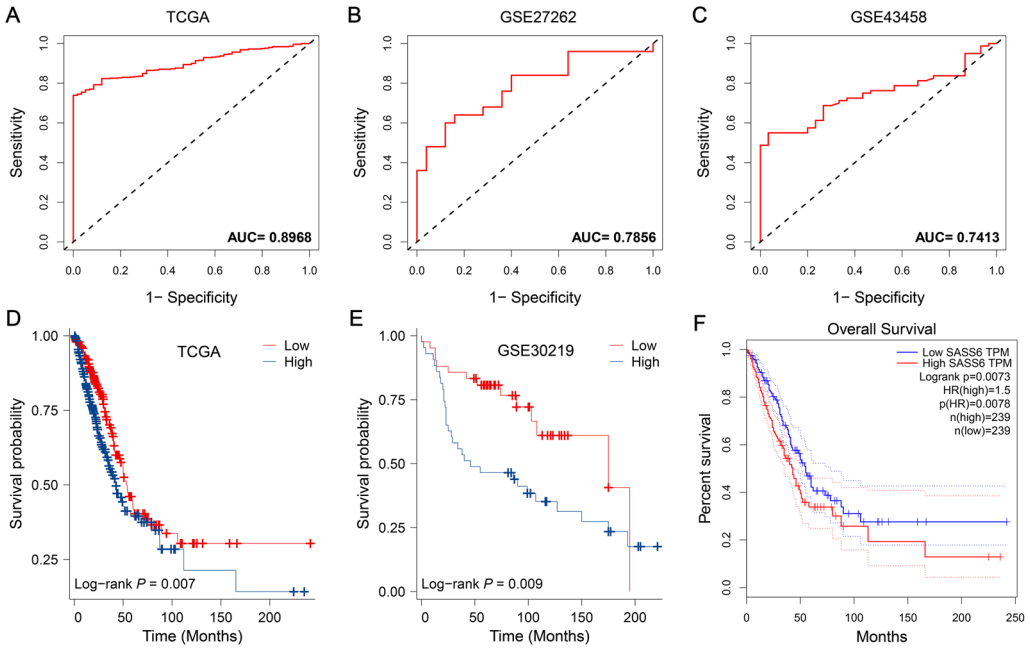

Fig. 4 Diagnostic efficiency and prognostic value of SASS6 in LUAD. **A–C** Diagnostic ROC curves constructed in relation to SASS6 expression in the TCGA, GSE27262, and GSE43458 datasets. **D–F** KM survival curve constructed by grouping according to the median expression of SASS6 from TCGA, GSE30219 dataset and GEPIA database

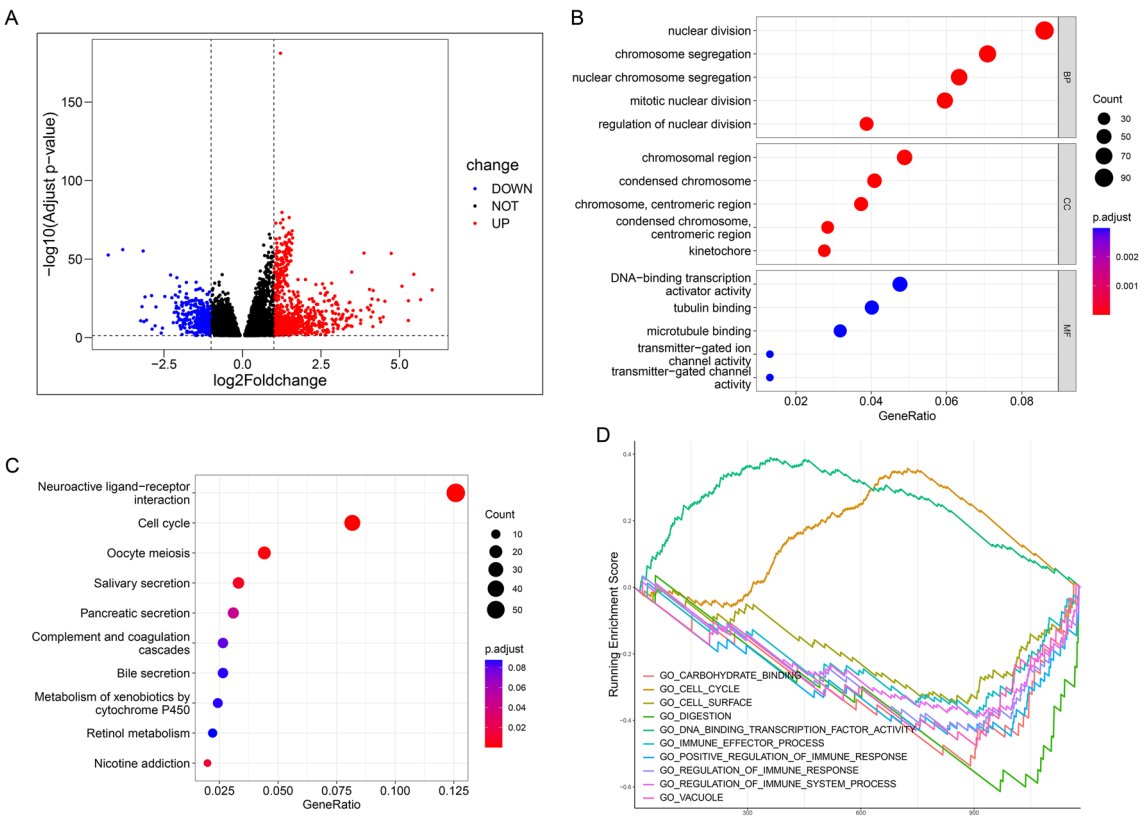

Fig. 5 Acquisition and function annotation of DEGs. **A** A volcano map constructed from significant DEGs in the TCGA dataset. **B** A dot plot showing the GO analysis results. **C** A dot plot showing the KEGG analysis results. The size and color of the dots represent the degree of gene enrichment and significance, respectively. **D** Demonstration of results acquired from GSEA analysis

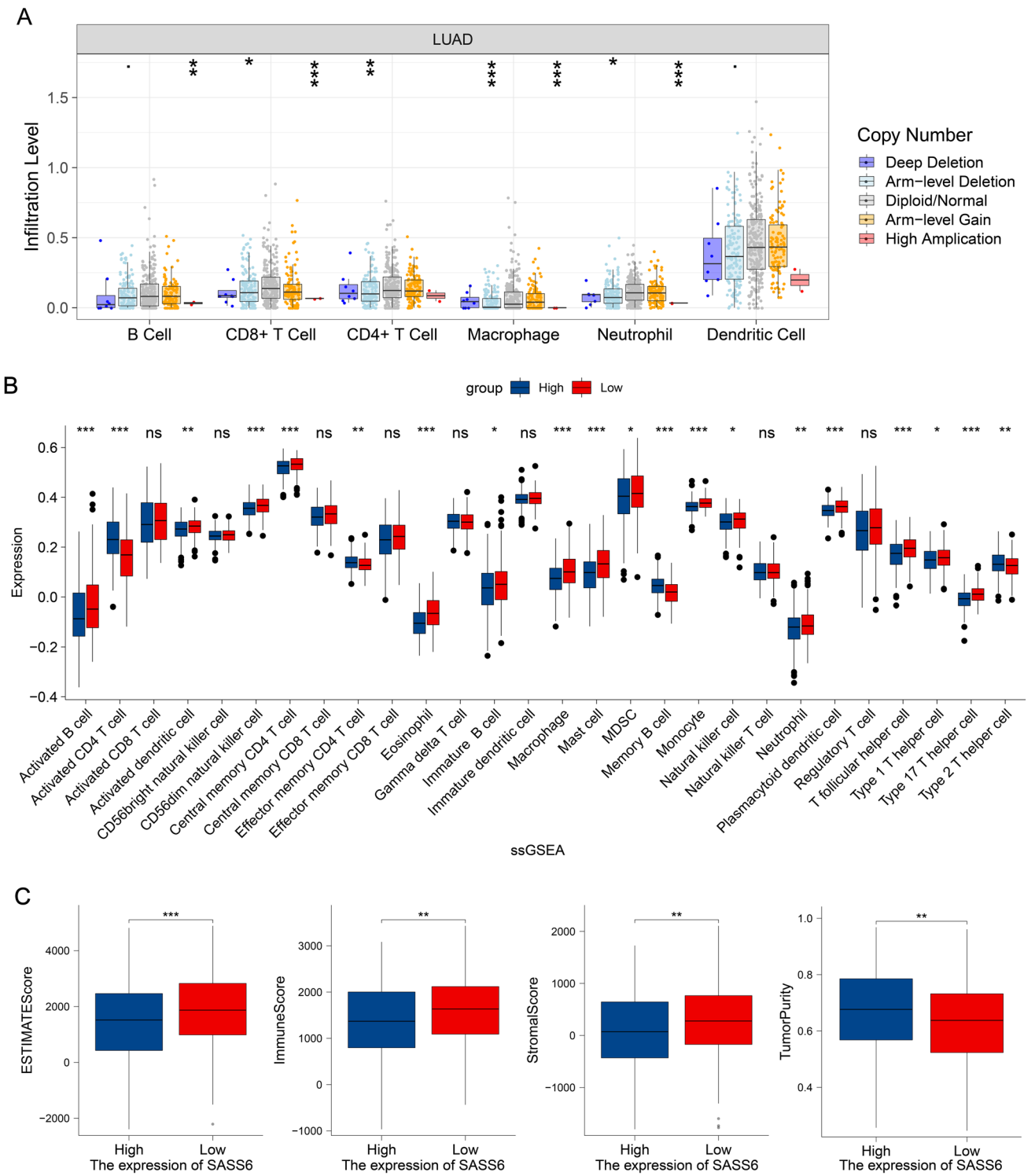

Fig. 6 Correlation analysis of immune infiltration associated with SASS6. **A** Analysis of immune cell infiltration levels between tumor cases with different SASS6 CNV in LUAD. CNV: copy number variation. **B** Differences in the expression of immune cells between two groups with different SASS6 expression. **C** Comparison of results obtained by ESTIMATE analysis

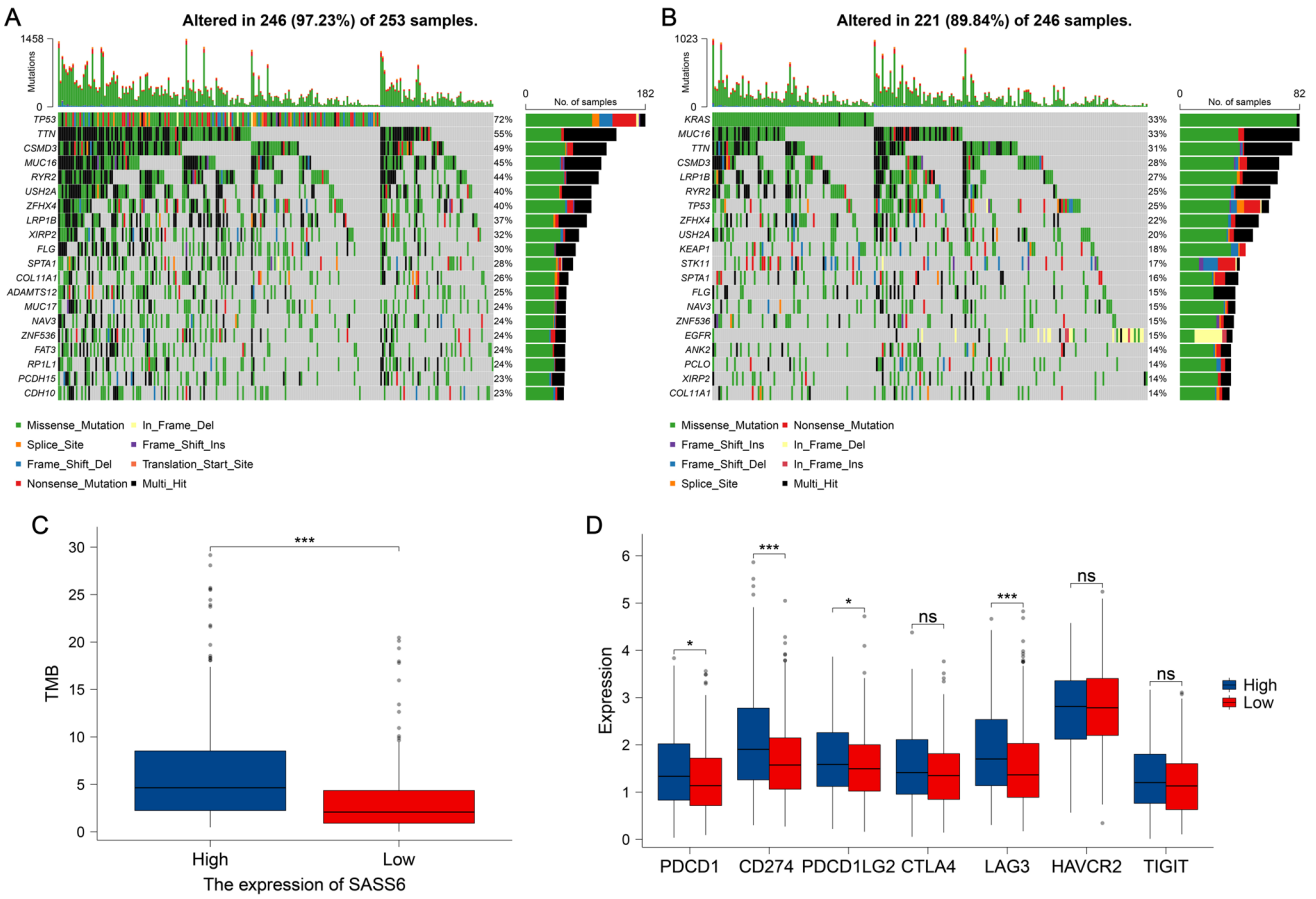

Fig. 7 Investigation of the association between SASS6 and immunotherapy. **A** Waterfall map of genetic mutations in samples with high SASS6 expression. **B** Waterfall map of genetic mutations in samples with low SASS6 expression. **C** Differences of TMB between the two groups with discrepant SASS6 expression. **D** Differential analysis of immune checkpoint expression

Construction of ceRNA network targeting SASS6

The predicted miRNA was hsa–let–7b–5p, which was negatively correlated with SASS6 (Fig. 9A). The lncRNAs predicted by hsa–let–7b–5p were CYP4F26P, AC087741.1, AC074117.1, and AC109460.3, which were negatively correlated with hsa–let–7b–5p (Fig. 9B–E). Through the construction of ceRNA network, the relationship between SASS6, hsa–let–7b–5p and lncRNAs (CYP4F26P, AC087741.1, AC074117.1, and AC109460.3) was shown (Fig. 9F). Compared with the normal group, hsa–let–7b–5p was highly expressed in the LUAD group (Fig. 9G), and its up-regulation suggested a better prognosis of LUAD (Fig. 9I). CYP4F26P was overexpressed in the LUAD group (Fig. 9H), and its up-regulation suggested a worse prognosis of LUAD (Fig. 9J). Both hsa–let–7b–5p and CYP4F26P were differentially expressed between LUAD and normal cases, and they contributed to the survival of tumor cases, so they were identified as core miRNA and core lncRNA, respectively.

Experimental validation of differential expression of SASS6 in LUAD

Immunohistochemistry results showed deeper staining in LUAD tumor tissues, confirming that SASS6 is overexpressed in LUAD (Fig. 10).

Biological function of SASS6 in lung cancer cells

The results of WB showed that SASS6 was highly expressed in lung cancer cells (Fig. 11A), and the expression of SASS6 was successfully knocked down for subsequent cell function experiments (Fig. 11B). CCK8 and EDU assays confirmed that SASS6 knockdown attenuated proliferation of lung cancer (Fig. 11C, D). Knockdown of SASS6 inhibited the migration and invasion of lung cancer through Transwell assay (Fig. 11E), and wound healing assay further confirmed that SASS6 knockdown reduced the migration ability of cancer cells (Fig. 11F).

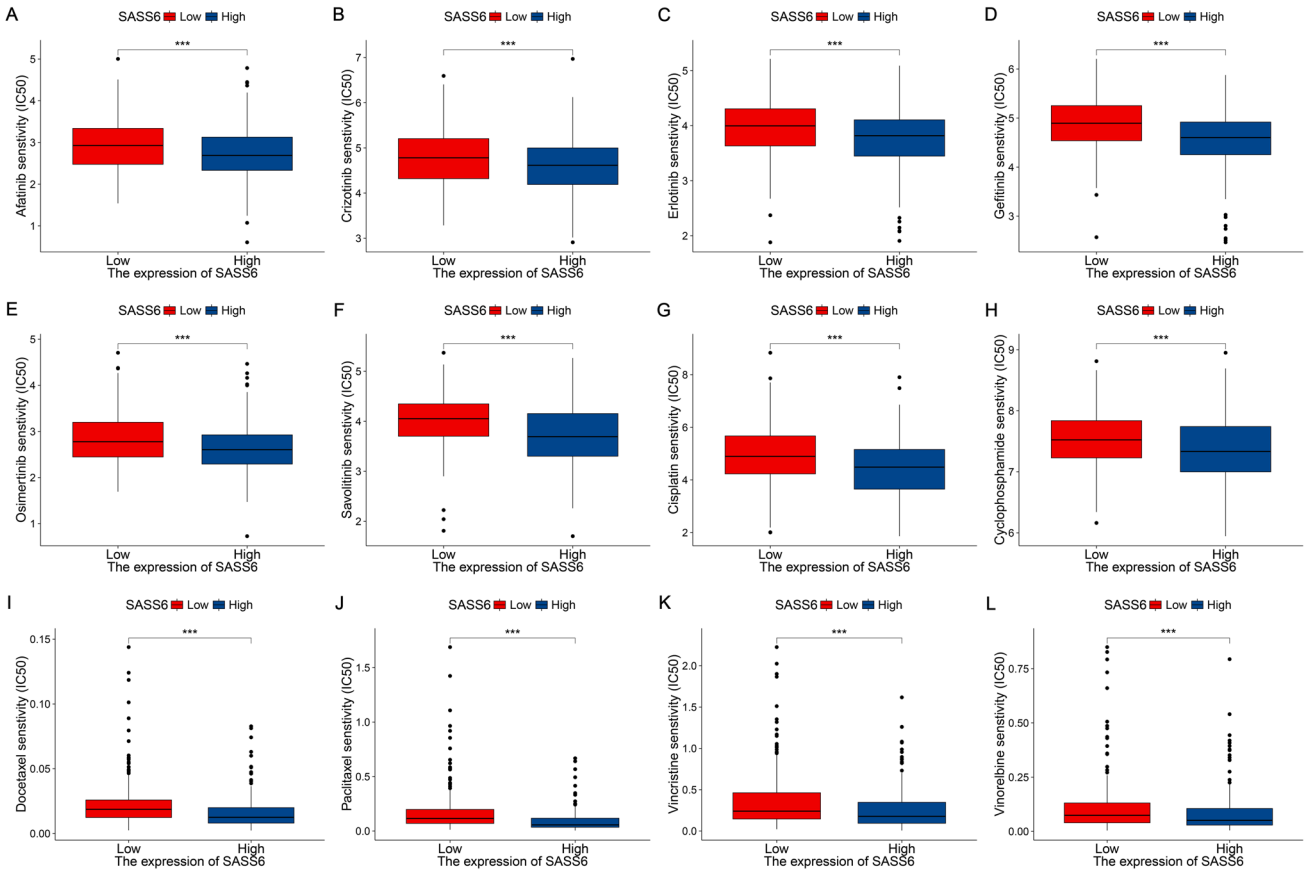

Fig. 8 Study on drug sensitivity in LUAD. **A** Analysis of difference in sensitivity of afatinib between high and low SASS6 expression groups. **B** Analysis of difference in sensitivity of crizotinib between two groups. **C** Analysis of difference in sensitivity of erlotinib between two groups. **D** Analysis of difference in sensitivity of gefitinib between two groups. **E** Analysis of difference in sensitivity of osimertinib between two groups. **F** Analysis of difference in sensitivity of savolitinib between two groups. **G** Analysis of difference in sensitivity of cisplatin between two groups. **H** Analysis of difference in sensitivity of cyclophosphamide between two groups. **I** Analysis of difference in sensitivity of docetaxel between two groups. **J** Analysis of difference in sensitivity of paclitaxel between two groups. **K** Analysis of difference in sensitivity of vincristine between two groups. **L** Analysis of difference in sensitivity of vinorelbine between two groups

Discussion

Chromosome stability is one of the important conditions for the orderly biological activities of cells, and the occurrence of tumors and abnormal immune cell infiltration are usually related to chromosome abnormalities [12, 17]. Centrosome amplification, that is, the presence of more than two centrosomes, interferes with the process of cell division, resulting in the increased probability of chromosome instability, thereby promoting the occurrence and progression of tumors [18]. Chromosomal instability, abnormal mitosis, and centrosome amplification can be induced by abnormal expression of SASS6 [10, 19, 20]. It has been previously revealed that overexpression of SASS6 is an important factor in the progression of several different types of cancer; for example, in colorectal cancer, overexpression of SASS6 is closely related to the pathogenesis of the tumor and is a risk factor for poor prognosis [21]. The role of SASS6 in LUAD has not been studied and reported previously. In this study, SASS6 was found to be overexpressed in 15 malignant tumors, including LUAD, and it is mainly expressed in cancer stem cells. In addition. In addition. SASS6 expression was applied to diagnose malignant tumors, and the procedures demonstrated satisfactory efficiency. Survival analysis revealed a grave prognosis in LUAD samples with SASS6 overexpression. Therefore, SASS6 was identified as a diagnostic and prognostic marker for LUAD.

This study suggested that SASS6 was significantly related to cell cycle and immune response, and may contributed to cancer progression in LUAD patients through these pathways. Tumorigenesis is regulated by a variety of basic mechanisms, and the abnormality of cell cycle progression is one of them [22]. Subsequently, experiments were designed to

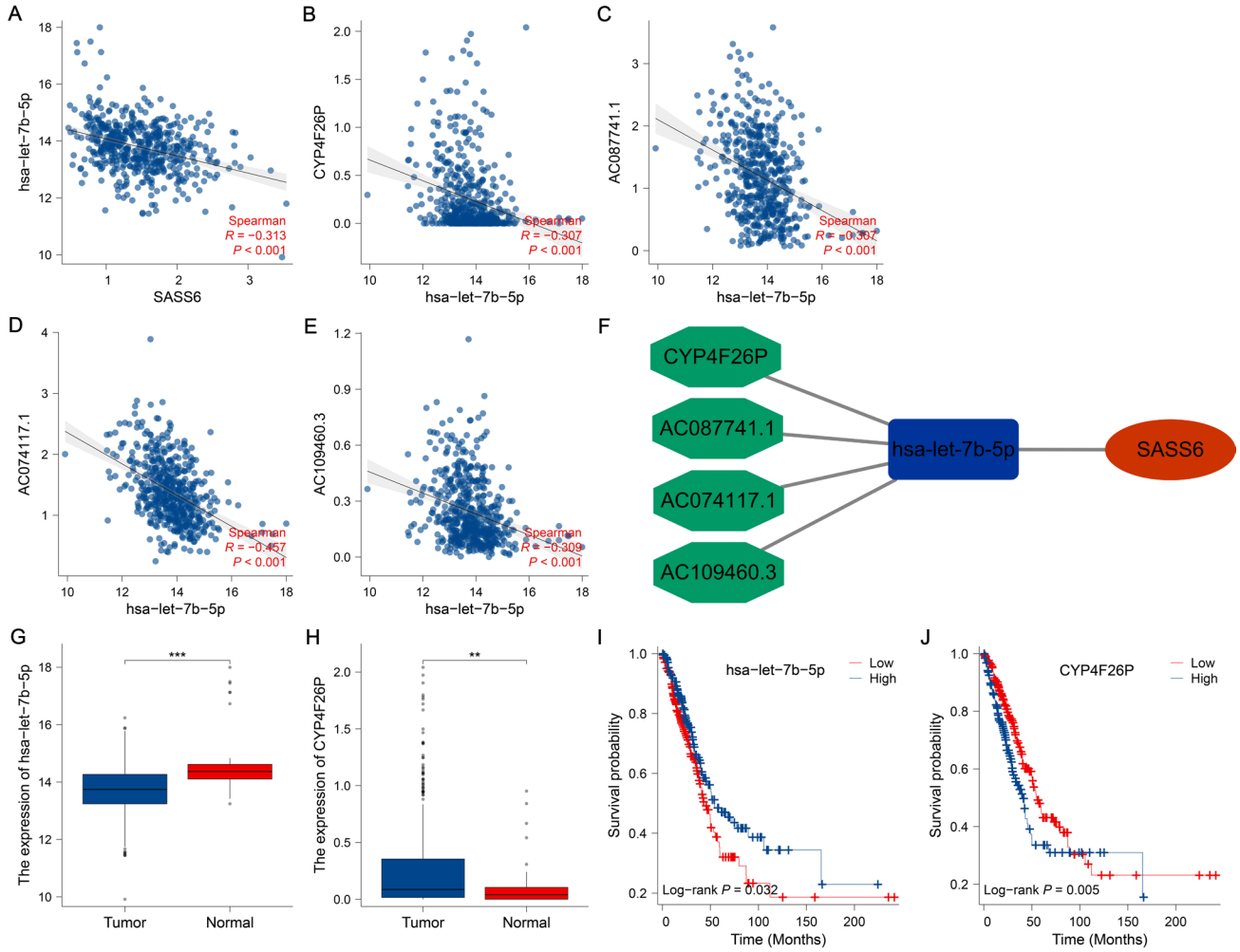

Fig. 9 Study on upstream gene of SASS6. **A** Correlation analysis between SASS6 and miRNA (hsa–let–7b–5p) predicted by SASS6. **B** Correlation analysis between hsa–let–7b–5p and lncRNA (CYP4F26P) predicted by hsa–let–7b–5p. **C** Analysis of correlation between hsa–let–7b–5p and lncRNA (AC087741.1) predicted by hsa–let–7b–5p. **D** Analysis of correlation between hsa–let–7b–5p and lncRNA (AC074117.1) predicted by hsa–let–7b–5p. **E** Analysis of correlation between hsa–let–7b–5p and lncRNA (AC109460.3) predicted by hsa–let–7b–5p. **F** CeRNA networks associated with SASS6. **G** Difference analysis of hsa–let–7b–5p between LUAD group and normal group. **H** Difference analysis of CYP4F26P between LUAD group and normal group. **I** KM survival analysis of hsa−let−7b−5p in LUAD cases. **J** KM survival analysis of CYP4F26P in LUAD cases

investigate the differential expression of SASS6 in LUAD. It was confirmed that SASS6 was up-regulated in LUAD, and SASS6 can promote the growth and development of tumor cells.

Tumor microenvironment is closely related to the occurrence and progression of tumors, and immune cells, as a part of it, play an indispensable role [23, 24]. A variety of immune cells were found to be down-regulated in SASS6 overexpression group. The arm-level of SASS6 was also found to be in connection with the infiltration of multiple immune cells, including B cell, CD8+ T cell, CD4+ T cell, Macrophage, neutrophil. As antigen presenting cells, B cells can differentiate into plasma cells, produce anti-tumor antibodies and promote T cell responses to enhance anti-tumor effects [25]. The indirect anti-tumor effect of CD4 T cells is achieved by promoting the anti-tumor effect of other anti-tumor effector cells, which is closely related to the anti-tumor response [26, 27]. Macrophages can be divided into two functionally opposite subtypes, M1 and M2, with M2 cells showing tumor-promoting effects [28]. Finally, we quantified the tumor microenvironment of each patient by ESTIMATE, and found that samples with high SASS6 expression had lower immune scores but higher tumor purity

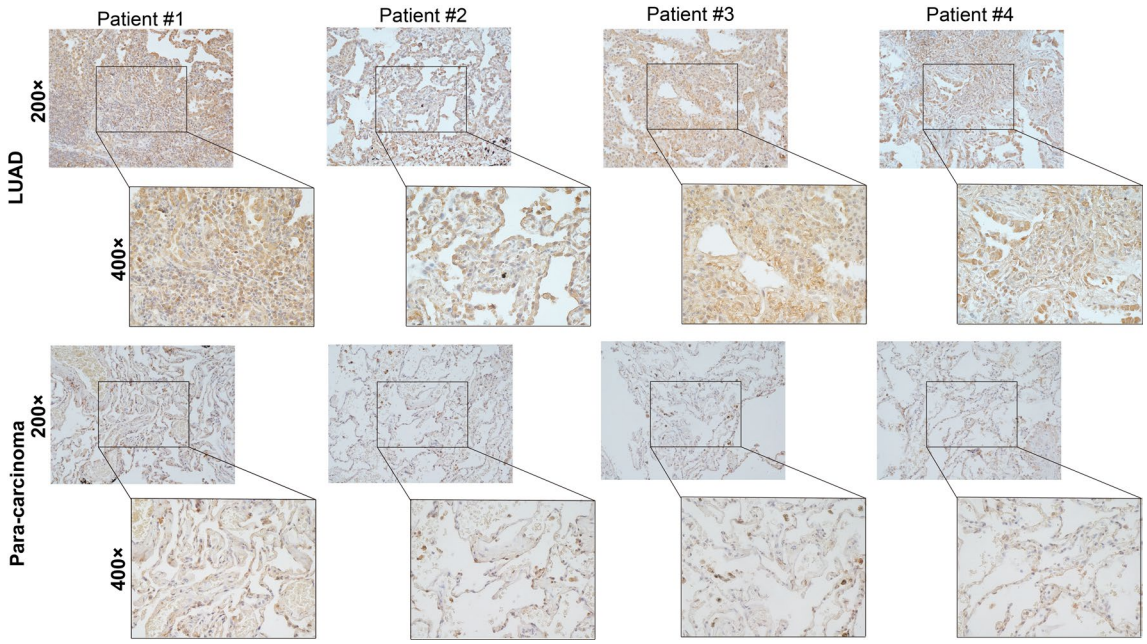

Fig. 10 The expression of SASS6 was up-regulated in LUAD. Immunohistochemical images of the tumor and adjacent lung tissue from 4 patients with LUAD

by grouping comparison. The above results indicated that high SASS6 expression in LUAD was related to low immune infiltration.

Cell cycle regulators may be potential therapeutic targets for cancer, and therapies targeting these genes can inhibit tumor cell division [29]. Afatinib, erlotinib and gefitinib, as the most widely used EGFR TKIs in NSCLC, are the first-line treatment regimens for EGFE mutation-positive lung adenocarcinoma, which have significant superiority in remission rates and progression-free survival [30, 31]. However, acquired drug resistance is one of the causes of poor prognosis in the treatment of NSCLC patients with EGFR-TKI, and the application of osimertinib is the standard treatment for drug-resistant NSCLC with T790M mutation [32]. Crizotinib, a first-generation anaplastic lymphoma kinase (ALK) inhibitor, is the standard first-line treatment for advanced ALK-positive NSCLC and is more effective than chemotherapy [33]. Savolitinib is used in advanced NSCLC with MET exon 14 skipping mutations, particularly those that are refractory to platinum-based chemotherapy regimens [34]. In this study, we found that LUAD samples with high expression of SASS6 showed higher sensitivity to these six targeted drugs and some common chemotherapeutic agents such as cisplatin. High TMB can increase the opportunity of T cells to recognize antigens, so that patients with high TMB show better efficacy in immunotherapy. In this study, SASS6 overexpression was associated with higher TMB and immune checkpoint gene, suggesting that patients with SASS6 overexpression may have better response to immunotherapy and are better candidates for immunological therapy to reestablish immune microenvironment. These findings suggest that SASS6 is a potential therapeutic target for LUAD and provide new insights into the clinical management of LUAD.

As a tumor suppressor gene, TP53 has the activity of encoding the p53 tumor suppressor protein, and the mutation of TP53 is the most common gene mutation in human cancers [35]. In our study, we found that the proportion of TP53 mutations was higher than 70% in LUAD samples with high SASS6 expression. TP53 mutation can up-regulate the expression level of immune checkpoint and predict the efficacy of immunological therapy [36]. These findings further highlight the relevance of SASS6 to immunotherapy and tumor progression.

In the ceRNA network, miRNA can specifically bind to the downstream mRNA and inhibit the translation process of mRNA, resulting in the reduction of protein production, while lncRNA can competitively bind to miRNA to reduce the binding of downstream mRNA to miRNA, thereby restoring the activity of mRNA [37, 38]. The ceRNA network regulates tumor initiation and progression through the above process. In this study, the lncRNA (CYP4F26P)

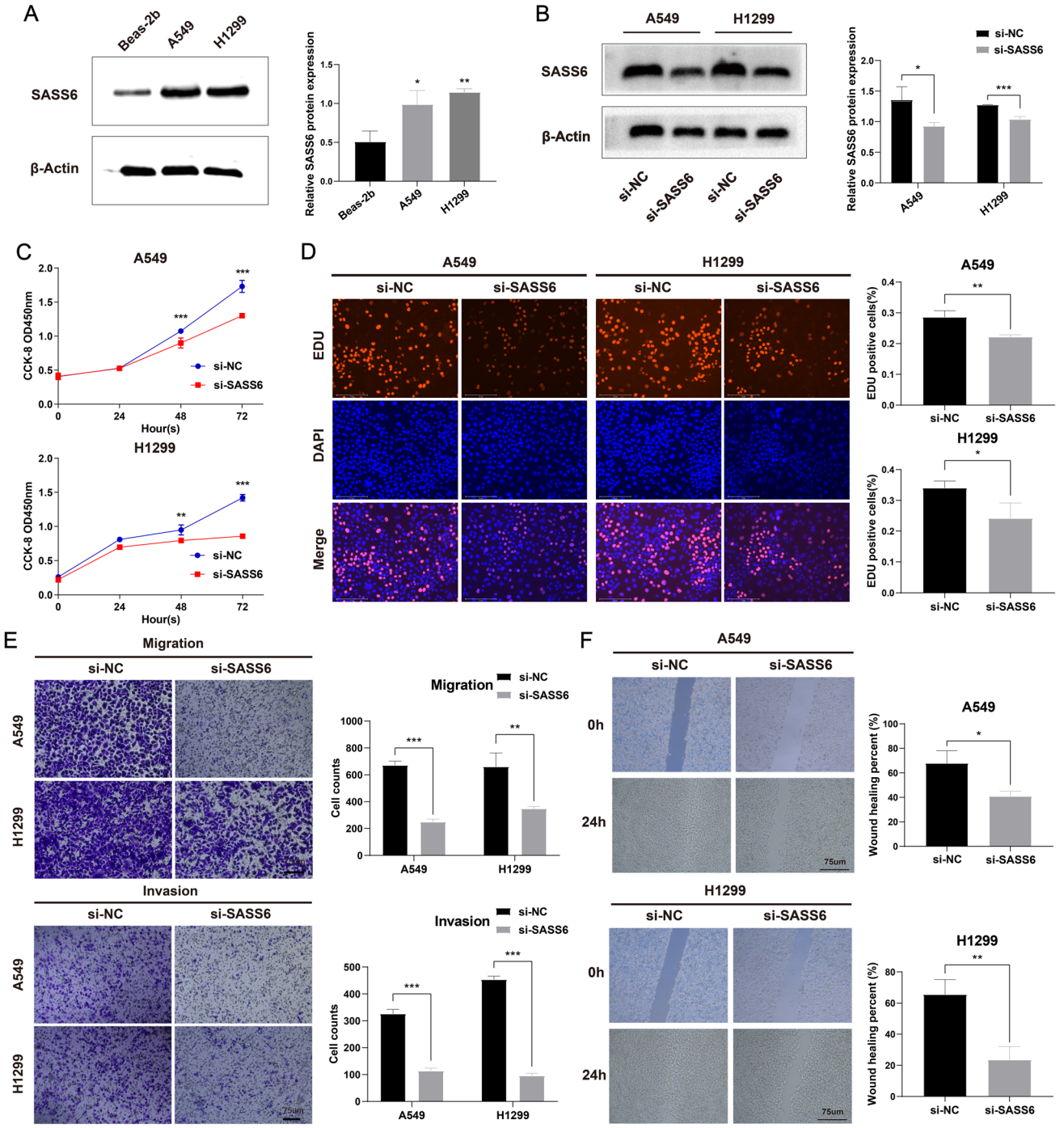

Fig. 11 SASS6 promoted tumor progression. **A** SASS6 protein was detected by WB in A549 and H1299 cells before RNA interference. **B** SASS6 protein was detected by WB in A549 and H1299 cells after RNA interference. The proliferation of tumor was detected by CCK8 (**C**) and EDU (**D**) assay in si-NC group and si-SASS6 group. **E** Transwell assay was implemented to verify the migration and invasion ability of A549 and H1299 cells. **F** Wound healing assay in tumor cells

-miRNA (hsa–let–7b–5p) -mRNA (SASS6) regulatory axis was obtained by prediction of ENCORI database and data analysis. It is speculated that the role of SASS6 in LUAD may be regulated by CYP4F26P and hsa–let–7b–5p.

Overall, our study explored the role of SASS6 in LUAD through the analysis of public databases and the implementation of cellular experiments. However, our study has certain limitations. First, the mechanism by which SASS6 regulates immune infiltration needs to be elucidated in animal

experiments. Secondly, the analysis of drug sensitivity needs to be confirmed by prospective trials.

Conclusions

SASS6 has remarkable diagnostic value in pan-cancer, and has prognostic and therapeutic value in LUAD, which can be developed as a novel biomarker. SASS6 may play a carcinogenic role in LUAD by adjusting cell cycle and immune infiltration.

Acknowledgements We would like to thank the public database (TCGA, GEO, TIMER, ENCORI, and HPA databases) and everyone involved in this study.

Author contributions Zihao Li, Lingyun He, Jing Qian, Ting Zhuo and Jusen Nong contributed to the conception and design. Zuotao Wu and Honghua Liang collected clinical data. Zihao Li, Jiayi Li, Yongjie Zhu and Hua Zheng analyzed the data. Zihao Li and Lingyun He wroted the manuscript. Julu Huang and Jianbin Cao revised and reviewed the final version of the manuscript. All authors contributed to the article and approved the submitted version.

Funding None.

Data availability The original data for this paper can be found in the UCSC Xena (xenabrowser.net), GEO database (https://www.ncbi.nlm.nih.gov/geo/), Genomic Data Commons (https://portal.gdc.cancer.gov/), miRbase (https://www.mirbase.org/). Relevant data for this study are also available upon request from the corresponding author. No datasets were generated or analysed during the current study.

Declarations

Conflicts of interest The authors declare that the research was conducted in the absence of any commercial or financial relationships that could be construed as a potential conflict of interest. The authors declare no competing interests.
Ethi

Ethical approval The experimental part of this study was approved by the Medical Ethics Committee of First Affiliated Hospital of Guangxi Medical University (Approval Number: 2023- E591-01), and informed consent was obtained from all patients who participated in this study. All methods were carried out in accordance with the Helsinki declaration guidelines and regulations.

References

1. Sung H, et al. Global cancer statistics 2020: GLOBOCAN estimates of incidence and mortality worldwide for 36 cancers in 185 countries. CA Cancer J Clin. 2021;71(3):209–49.
2. Siegel RL, et al. Cancer statistics, 2023. CA Cancer J Clin. 2023;73(1):17–48.
3. Goldstraw P, et al. The IASLC lung cancer staging project: proposals for revision of the TNM stage groupings in the forthcoming (Eighth) edition of the TNM classification for lung cancer. J Thorac Oncol. 2016;11(1):39–51.
4. Thai AA, et al. Lung cancer. Lancet. 2021;398(10299):535–54.
5. Chaft JE, et al. Evolution of systemic therapy for stages I-III non-metastatic non-small-cell lung cancer. Nat Rev Clin Oncol. 2021;18(9):547–57.
6. Xu JY, et al. Integrative proteomic characterization of human lung adenocarcinoma. Cell. 2020;182(1):245-261.e17.
7. Wang ZF, et al. Frequency of the acquired resistant mutation T790 M in non-small cell lung cancer patients with active exon 19Del and exon 21 L858R: a systematic review and meta-analysis. BMC Cancer. 2018;18(1):148.
8. Memon H, Patel BM. Immune checkpoint inhibitors in non-small cell lung cancer: a bird's eye view. Life Sci. 2019;233: 116713.
9. Yang CY, Yang JC, Yang PC. Precision management of advanced non-small cell lung cancer. Annu Rev Med. 2020;71:117–36.
10. Leidel S, et al. SAS-6 defines a protein family required for centrosome duplication in C. elegans and in human cells. Nat Cell Biol. 2005;7(2):115–25.
11. Doxsey S. The centrosome–a tiny organelle with big potential. Nat Genet. 1998;20(2):104–6.
12. Kou F, et al. Chromosome abnormalities: new insights into their clinical significance in cancer. Mol Ther Oncolytics. 2020;17:562–70.
13. Kawamura K, et al. Induction of centrosome amplification and chromosome instability in human bladder cancer cells by p53 mutation and cyclin E overexpression. Cancer Res. 2004;64(14):4800–9.
14. Du L, et al. Knockdown of SASS6 reduces growth of MDA-MB-231 triple-negative breast cancer cells through arrest of the cell cycle at the G2/M phase. Oncol Rep. 2021;45(6):1–10.
15. Xu Y, et al. SASS6 promotes proliferation of esophageal squamous carcinoma cells by inhibiting the p53 signaling pathway. Carcinogenesis. 2021;42(2):254–62.
16. Li T, et al. TIMER: A Web Server for Comprehensive Analysis of Tumor-Infiltrating Immune Cells. Cancer Res. 2017;77(21):e108–10.
17. Attaran-Bandarabadi F, et al. Loss of heterozygosity on chromosome 5 in Iranian esophageal cancer patients. Genet Mol Res. 2011;10(4):2316–25.
18. Fukasawa K. Centrosome amplification, chromosome instability and cancer development. Cancer Lett. 2005;230(1):6–19.
19. Yoshiba S, et al. HsSAS-6-dependent cartwheel assembly ensures stabilization of centriole intermediates. J cell sci. 2019;132(12):jcs217521.
20. Comartin D, et al. CEP120 and SPICE1 cooperate with CPAP in centriole elongation. Curr Biol. 2013;23(14):1360–6.
21. Shinmura K, et al. SASS6 overexpression is associated with mitotic chromosomal abnormalities and a poor prognosis in patients with colorectal cancer. Oncol Rep. 2015;34(2):727–38.
22. Jamasbi E, et al. The cell cycle, cancer development and therapy. Mol Biol Rep. 2022;49(11):10875–83.
23. Belli C, et al. Targeting the microenvironment in solid tumors. Cancer Treat Rev. 2018;65:22–32.
24. Wang M, et al. Tumor-microenvironment-activated reactive oxygen species amplifier for enzymatic cascade

cancer starvation/chemodynamic /immunotherapy. Adv Mater. 2022;34(4):e2106010.
25. Tokunaga R, et al. B cell and B cell-related pathways for novel cancer treatments. Cancer Treat Rev. 2019;73:10–9.
26. Zander R, et al. CD4(+) T cell help is required for the formation of a cytolytic CD8(+) T cell subset that protects against chronic infection and cancer. Immunity. 2019;51(6):1028-1042.e4.
27. Oh DY, Fong L. Cytotoxic CD4(+) T cells in cancer: expanding the immune effector toolbox. Immunity. 2021;54(12):2701–11.
28. Najafi M, et al. Macrophage polarity in cancer: a review. J Cell Biochem. 2019;120(3):2756–65.
29. Liu J, Peng Y, Wei W. Cell cycle on the crossroad of tumorigenesis and cancer therapy. Trends Cell Biol. 2022;32(1):30–44.
30. Köhler J, Schuler M. Afatinib, erlotinib and gefitinib in the first-line therapy of EGFR mutation-positive lung adenocarcinoma: a review. Onkologie. 2013;36(9):510–8.
31. Yang Z, et al. Comparison of gefitinib, erlotinib and afatinib in non-small cell lung cancer: a meta-analysis. Int J Cancer. 2017;140(12):2805–19.
32. Tamiya M, et al. Which Is Better EGFR-TKI Followed by Osimertinib: Afatinib or Gefitinib/Erlotinib? Anticancer Res. 2019;39(7):3923–9.
33. Shaw AT, et al. First-line lorlatinib or crizotinib in advanced ALK-positive lung cancer. N Engl J Med. 2020;383(21):2018–29.
34. Markham A. Savolitinib: first approval. Drugs. 2021;81(14):1665–70.
35. Hassin O, Oren M. Drugging p53 in cancer: one protein, many targets. Nat Rev Drug Discov. 2023;22(2):127–44.
36. Biton J, et al. TP53, STK11, and EGFR mutations predict tumor immune profile and the response to Anti-PD-1 in lung adenocarcinoma. Clin Cancer Res. 2018;24(22):5710–23.
37. Karreth FA, Pandolfi PP. ceRNA cross-talk in cancer: when ce-bling rivalries go awry. Cancer Discov. 2013;3(10):1113–21.
38. Qi X, et al. ceRNA in cancer: possible functions and clinical implications. J Med Genet. 2015;52(10):710–8.